ARMA 12-290

Shear Strength Anisotropy in Fine-grained Rocks

Crawford, B.R.
ExxonMobil Upstream Research Company, Houston, TX, USA
DeDontney, N.L. and Alramahi, B.
ExxonMobil Upstream Research Company, Houston, TX, USA
Ottesen, S.
ExxonMobil Development Company, Houston, TX, USA

This paper was prepared for presentation at the 46th US Rock Mechanics / Geomechanics Symposium held in Chicago, IL, USA, 24-27 June 2012. This paper was selected for presentation at the symposium by an ARMA Technical Program Committee based on a technical and critical review of the paper by a minimum of two technical reviewers. The material, as presented, does not necessarily reflect any position of ARMA, its officers, or members. Electronic reproduction, distribution, or storage of any part of this paper for commercial purposes without the written consent of ARMA is prohibited. Permission to reproduce in print is restricted to an abstract of not more than 300 words; illustrations may not be copied. The abstract must contain conspicuous acknowledgement of where and by whom the paper was presented.

ABSTRACT: Significant strength anisotropy associated with weak bedding laminations can lead to wellbore instability issues when drilling inclined wells through shale formations. We have compiled a database of ≈400 orientated triaxial compression tests in 14 lithologies (mainly argillaceous shales and calcareous marls) to quantify the magnitude of strength anisotropy likely to be encountered *in situ*. All data is analyzed using both discontinuous single plane of weakness and continuously variable strength models. Anisotropy is primarily found to result from a systematic dependency of cohesive strength on orientation angle compared with the more random variation of internal friction which is most likely due to material inhomogeneity. Cohesive strength reduction (shearing through versus shearing along weak laminations) ranges from ≈20–80% depending on lithology. From our database analyses we observe systematically higher reduction (hence greater anisotropy) in the weaker fine-grained rocks.

1. INTRODUCTION

As noted by Sondergeld & Rai [1] "shales are now universally recognized as being anisotropic." Knowledge of shale anisotropy has been significantly advanced by the geophysics community through the need for understanding seismic wave propagation (incorporating anisotropy into migration algorithms allows for proper positioning of reflectors, [2]) such that the majority of experimental and theoretical investigations have focused on the elastic properties of shales (e.g. [3], [4]). The elastic anisotropy of many shales encountered in the subsurface can be described, to a good approximation, as being transversely isotropic with a vertical axis of rotational symmetry [5]. Such vertical transversely isotropic "VTI" media possess 5 independent elastic stiffnesses and 3 anisotropy parameters denoted by "ε", "γ" and "δ" [6] where "ε" and "γ" have a simple interpretation in terms of the wave velocities for propagation parallel and perpendicular to the symmetry axis. A compilation of over 150 shale anisotropy experiments [1] indicate that most measured "ε"and "γ" magnitudes are greater than 10% and can approach 50-60% indicating that elastic anisotropy in shales is "strong."

The origin of elastic/seismic anisotropy in shales is non-unique and has been attributed to a multiplicity of factors [7] including "intrinsic" texture associated with single crystal properties and the preferred orientation of clay mineral platelets resulting from slow sedimentation [8] augmented with microcracks [9] and stress-induced anisotropy [10]. This pattern is modified during compaction and diagenesis [11]. During compaction shale density increases and clay particles become progressively more aligned suggesting that shale density and anisotropy should be positively correlated. However experimental evidence indicating that anisotropy increases with organic matter content [12] would produce an effect opposite to compaction as density and particle alignment decrease with increasing organics.

By comparison with the relatively advanced understanding of elastic anisotropy in shales, research into shale strength anisotropy has received much less attention. This observation may partly reflect the fact that many more test samples are required to quantify strength as opposed to elastic anisotropy (see discussion in Section 3). Nevertheless, numerous experimental studies have sought to investigate the mechanical behavior of rocks with strong planar geologic fabrics including: slate [13], [14], [15]; schist and gneiss [16], [17], [18]; shale and mudstone [13], [19], [20], [21], [22], [23]; siltstone [24]; sandstone [20]; limestone [25]; and coal [26]. While strength anisotropy has importance in structural geology as frictional slip along relatively weak bedding planes contributes to the deformation of layered rocks [27] interest in shale strength anisotropy has resulted primarily from a desire to understand

wellbore failure mechanisms associated with drilling through shales. Although elastic anisotropy in shales can impact wellbore failure through the redistribution of borehole stresses, analytical studies have shown that strength anisotropy has a more important control [28]. This effect is particularly pronounced for extended reach drilling where the borehole trajectory can achieve near-parallelism with weak bedding planes (shown schematically in Fig. 1).

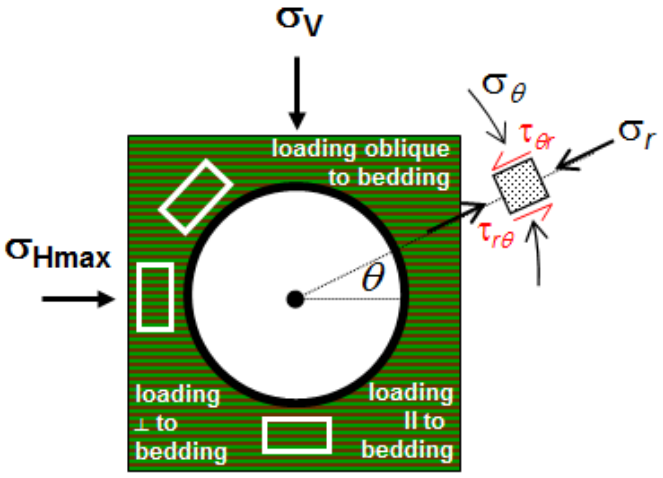

Fig. 1. Near-wellbore stresses with respect to shale anisotropy in a horizontal wellbore.

If the attack angle is low (≈70-90° borehole inclination through a formation with ≈0° dip angle) interaction between the borehole hoop stress "σ_θ" and the anisotropic formation can result in oblique loading of the relatively weak bedding laminations leading to premature shear failure. This failure mechanism is often wrongly attributed to the invasion of drilling fluids into micro-fractures along bedding planes [29]. Depending on the relative magnitudes of anisotropic rock strength and borehole stress concentration, breakouts may occur at "unexpected" positions around the borehole different from those conventionally found in isotropic rock [30]. Geographically-diverse examples of anisotropic rock strength models being used to optimize drilling programs include: Gulf of Mexico [31], [32]; Canada [33], [34]; Venezuela and Colombia [35]; and the UK continental shelf [36].

In this study we aim to address two basic questions relating to the anisotropic strength of shales:

- What is the relative magnitude of strength anisotropy (shearing along versus shearing through weak bedding laminations) likely to be encountered in shale formations?
- Can strength anisotropy be estimated from conventional strength measurements in which laminations are orientated perpendicular to the direction of maximum compressive stress?

2. ANISOTROPIC STRENGTH THEORY

Numerous strength criteria have been proposed to capture the deformation behavior of anisotropic rocks under different loading conditions. Duveau *et al* [37] summarize many of these criteria and categorize them into distinct groups. The first includes discontinuous criteria such as the single plane of weakness "SPW" theory that we examine here (Jaeger [38]). In criteria of this form there is a distinction between failure on a weak plane (such as a bedding or lamination plane) and failure of the bulk material (where the failure surface cuts through planes of weakness). With this theory the strength of the rock is uniform with respect to orientation if the failure does not occur on a weak plane and variable if it does. Other discontinuous criteria include that of Walsh and Brace [39] which is a modification of Griffith theory in which anisotropy is assumed to be the result of a preferred orientation of cracks in the rock.

Another category of failure criteria includes those models which describe a continuous variation in strength with orientation such as Jaeger's [38] variable cohesive strength "VCS" theory which we examine here. For continuous models there is no implicit distinction between failure on a weak plane and failure of the bulk material. Starting from a strength value at bedding oriented perpendicular to loading, as the orientation of the planar anisotropy increases the strength gradually decreases until a distinct minimum is reached followed by strength recovery. Based on the shape of such strength versus orientation angle curves Ramamurthy [40] classified anisotropic response into 3 groups: U-type anisotropy; shoulder-type anisotropy; undulatory-type anisotropy. Other examples of empirical continuous models for shear failure of anisotropic rocks include those of Ramamurthy *et al.* [41] and Hoek & Brown [42]. Continuous models can be further subdivided into those that are an empirical fit to the variation of strength with orientation (such as the "VCS" model) and those with a yield criterion based on a mathematical formulation (such as a strength tensor). The yield criterion of Pariseau [43] is an example of the latter that allows for anisotropy and pressure dependence via coefficients that depend on the strength of the material in different orientations. Additional models have been developed such as the soft rock model of Crook *et al* [44] which is a modified form of the Cam Clay material model to allow for elastic-plastic deformation in transversely isotropic materials such as shales. In this formulation a modified stress state is determined based on the anisotropic properties and used to evaluate yield and plastic-flow characteristics.

In addition to the "SPW" theory we consider the original continuous "VCS" model of Jaeger and a modified version to empirically fit experimental strength data. The

original "VCS" model assumes that cohesive strength variation w.r.t. the orientation of planar features can be fit with a periodic cosine function and that the friction angle is constant w.r.t. orientation. McLamore & Gray [13] expanded upon this model by postulating additional periodic variation in friction angle with orientation and allowing both cohesion and friction angle to have dependence on a cosine function raised to a power. We do not utilize the McLamore & Gray adaptation but instead implement a modified "VCS" model that assumes a constant coefficient of friction and a third-order polynomial fit to cohesive strength variation w.r.t. orientation angle (rather than a cosine) to better reproduce the range in observed experimental behavior.

3. ANISOTROPIC STRENGTH DATABASE

The most common approach for characterizing elastic anisotropy in shales is to assume a symmetry axis, extract oriented plugs, and measure the phase velocities corresponding to specific elastic constants [1]. As shown in Fig. 2(a) for the assumption of "VTI" symmetry this requires plugging in horizontal, vertical, and 45° directions with respect to bedding in order to determine the five required elastic constants.

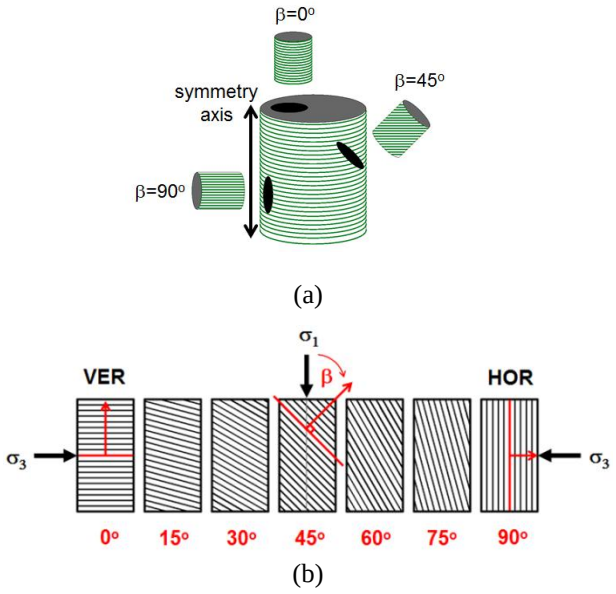

Fig. 2. Orientated core plug requirements for characterizing: (a) elastic anisotropy; (b) strength anisotropy in shales.

As illustrated in Fig. 2(b) experimental studies designed to quantify continuous variation in strength with orientation angle "β" (defined as the angle between the normal to the planar layering and the direction of maximum compressive stress "σ_1") have most often utilized plugs cored in 15° increments from the vertical (β =0°) to the horizontal (β =90°) direction such that a total of 7 core plugs are required for each lithology. As multiple additional plugs are also necessary for each orientation angle in order to determine strengthening associated with elevated confining pressure "σ_3" it is apparent that complete characterization of strength anisotropy can require an order of magnitude more core tests than equivalent characterization of elastic anisotropy.

To investigate the potential range in magnitude of strength anisotropy exhibited by diverse shale formations we have conducted an extensive experimental program of orientated triaxial compression testing on 7 individual lithologies (3 top seal shales, 3 intra-reservoir shales and 1 outcrop shale). To augment this database we have incorporated equivalent data sourced from the public domain, including: (i) lean (≈84liters per metric ton) and rich (≈165liters per metric ton) Green River Formation oil shale composed of fine-grained calcite and dolomite laminations interlayered with organic kerogen, (McLamore & Gray [13]); (ii) upper Toarcian Tournemire massive shale, (Niandou *et al* [19]); (iii) Carboniferous laminated silty mudstone, (Attewell & Farmer [23]). These 11 shale lithotypes can be broadly subdivided into argillaceous shales (varying amounts of clay minerals and silt-size quartz) versus calcareous shales or "marls" (varying amounts of clay and carbonate minerals). For comparative purposes we also analyze: (i) a Lower Devonian laminated dolomitic limestone composed of 0.25-1mm thick laminae of calcite pellets (with interstitial sparry calcite and scattered dolomite rhombs) and up to 10% nearly pure sparry dolomite laminae, (McGill & Raney [25]); (ii) a Pennsylvanian Age fine-grained, highly cemented sandstone, (Chenevert & Gatlin [20]); (iii) a dull bituminous coal with well-defined bedding planes and 2 orthogonal cleat directions, (Pomeroy *et al* [26]).

A summary of all 14 database lithologies (combined total of ≈400 triaxial compression tests) including Mohr-Coulomb strength parameters (cohesion "τ_0" and internal friction angle "φ") measured perpendicular to bedding (β =0°) is given in Table 1. We use the outcrop shale (#8 in Table 1) tested in-house to illustrate typical variation in observed peak strength as a function of orientation angle. In Fig. 3 complete stress difference (σ_1 – σ_3) versus (axial and radial) strain curves are shown for 35 triaxial compression tests (5 confining pressures, $3.45 \leq \sigma_3 \leq 68.9$MPa) in which orientation angle varies in 15° increments in the range $0° \leq \beta \leq 90°$. Peak strengths at equivalent confining pressures appear consistently lower for β= 45° and 60° orientation angles compared with other orientations. Post-test sample photographs (Fig. 4) suggest that these strength minima correlate with orientation angles for which induced shear fractures exhibit alignment with the plane of intrinsic anisotropy representing the orientation angles most favorable for failure.

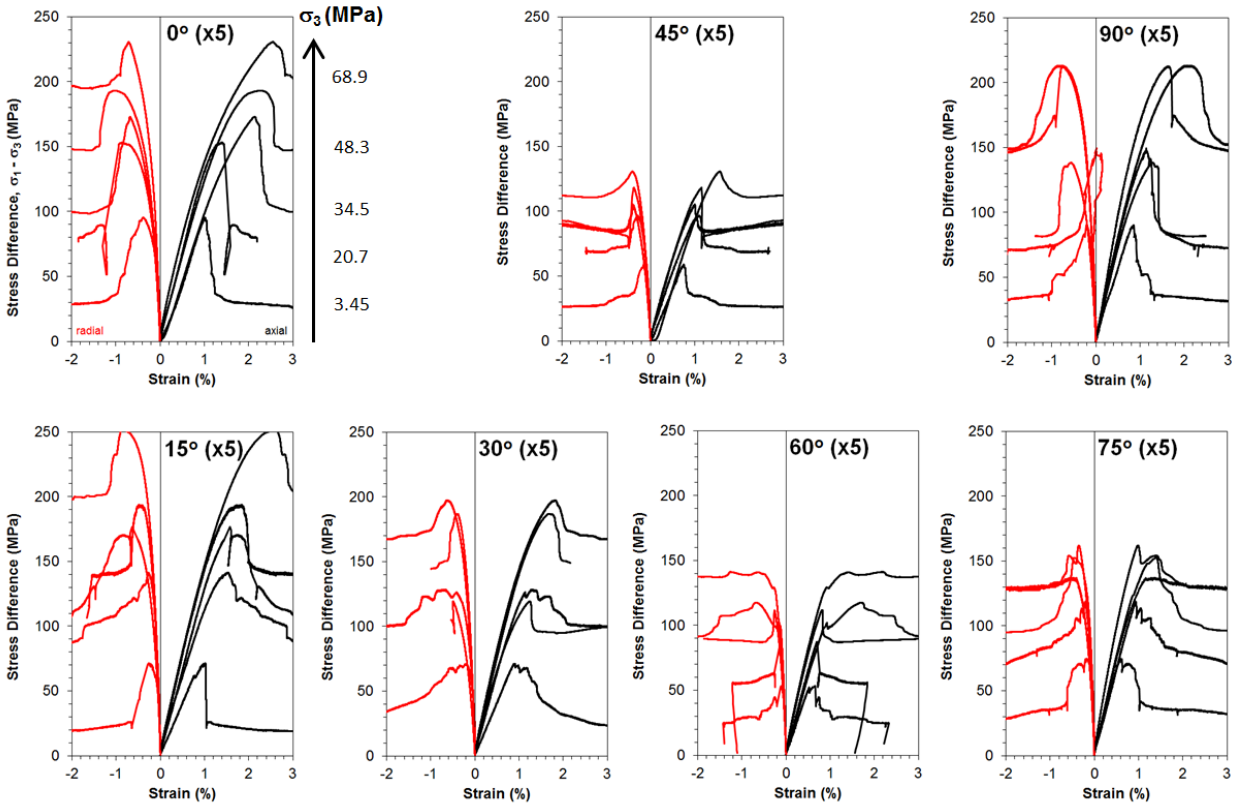

Fig. 3. Complete stress versus strain curves for orientated triaxial compression testing of outcrop shale (#8). 35 tests for 7x orientation angles in the range $0^o \leq \beta \leq 90^o$ (15^o increments) conducted at 5x confining pressures from 3.45 to 68.9MPa.

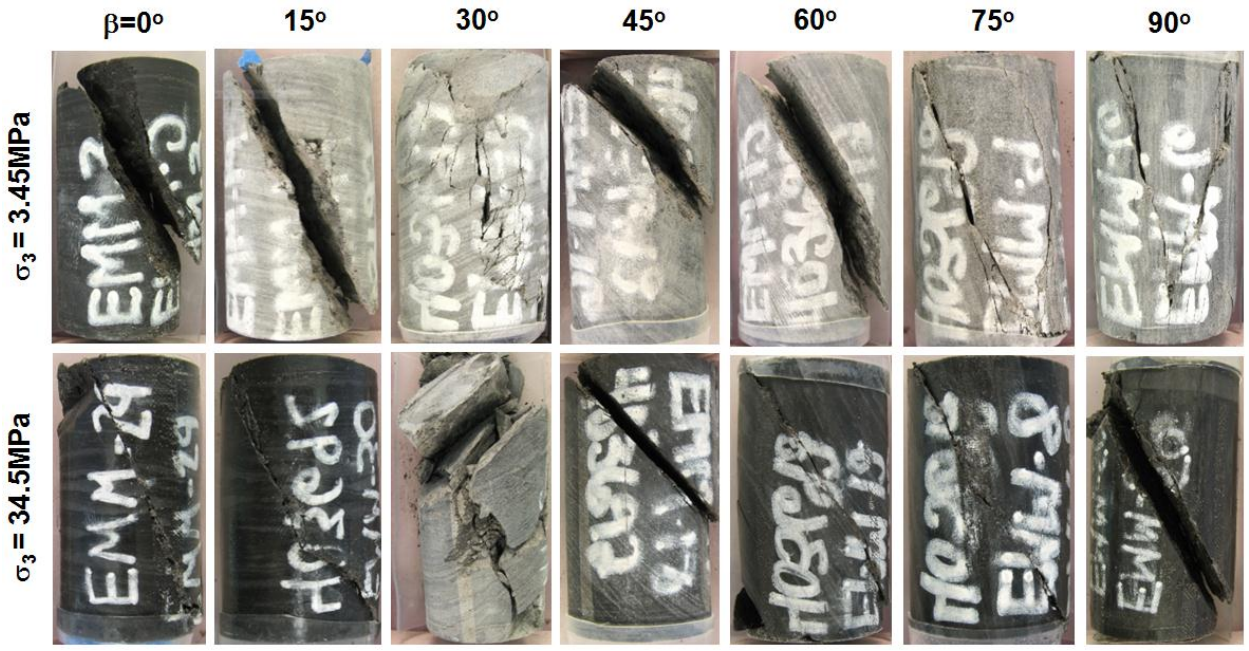

Fig. 4. Post-test sample photographs for orientated triaxial compression testing of outcrop shale (#8) illustrating induced shear fracture morphology. 10 tests for 7x orientation angles in the range $0^o \leq \beta \leq 90^o$ (15^o increments) conducted at 2x confining pressures of 3.45 and 34.5MPa.

Table 1. Summary of 14 database lithologies (≈400 triaxial compression tests) used in anisotropic shear strength analyses.

					$0 \le \beta(^o) \le 90$ # triaxial tests	Cohesive Strength $\tau_0 \mid_{\beta=0}$ (MPa)	Friction Angle $\varphi \mid_{\beta=0}$ (degrees)
	I.D.	Lithology		Source			
Lst.	#1	laminated dolomitic limestone	outcrop	McGill & Raney [25]	40	93.9	29.9
calcareous shales	#2	Green River oil shale (lean)	mine	McLamore &Gray [13]	24	59.6	31.4
	#3	Green River oil shale (rich)	"	"	21	39.0	21.4
	#4	intra-reservoir marl	cored well	in-house study	27	30.7	20.2
	#5	"	"	"	28	24.4	8.1
	#6	"	"	"	31	20.7	8.5
Sst.	#7	fine-grained highly cemented sandstone	outcrop	Chenevert & Gatlin [20]	17	38.4	56.4
argillaceous shales	#8	outcrop shale	"	in-house study	35	29.1	29.7
	#9	top seal shale	cored well	"	31	18.7	9.1
	#10	"	"	"	30	17.6	5.7
	#11	"	"	"	28	16.4	14.8
	#12	Tournemire shale	outcrop	Niandou *et al* [19]	25	16.8	21.7
	#13	laminated silty mudstone	mine	Attewell & Farmer [23]	42	14.9	33.8
Coal	#14	Barnsley Hards bituminous coal	mine	Pomeroy *et al* [26]	28	12.6	36.3
				Total # tests:	**407**		

4. ANISOTROPIC STRENGTH MODELING

4.1. Single Plane of Weakness

The single plane of weakness "SPW" [38] strength model is fully described using 4 material parameters: two cohesions "τ_0^b" and "τ_0^w"; two friction angles "φ^b" and "φ^w". It assumes that there is a weak plane in the bulk material at a specific orientation (see Fig. 5). The weak plane has strength properties "τ_0^w" and "φ^w" and if properly aligned with the principal stress axes failure occurs by slip on the plane. If the plane is not optimally aligned failure occurs within the bulk material and cuts across the plane of weakness. It is assumed that the bulk material has isotropic strength properties "τ_0^b" and "φ^b".

Failure will occur on the plane of weakness if:

$$|\tau| = \tau_0^w + \sigma_n \tan \varphi^w \qquad (1)$$

where the shear stress "τ" and normal stress "σ_n" on the plane are determined by the maximum and minimum principal stresses "σ_1" and "σ_3" respectively and the planar orientation angle "β" which is the angle between the σ_1-axis and the unit normal to the bedding plane (see Fig. 2(b)). Stresses on the plane are found via:

$$\tau = -\frac{1}{2}(\sigma_1 - \sigma_3)\sin 2\beta \qquad (2)$$

$$\sigma_n = \frac{1}{2}(\sigma_1 + \sigma_3) + \frac{1}{2}(\sigma_1 - \sigma_3)\cos 2\beta \qquad (3)$$

Substituting Eq. 2 and Eq. 3 into Eq. 1 enables determination of the maximum principal stress sustainable by the plane of weakness for a given orientation "β" before failure (see Eq. 4).

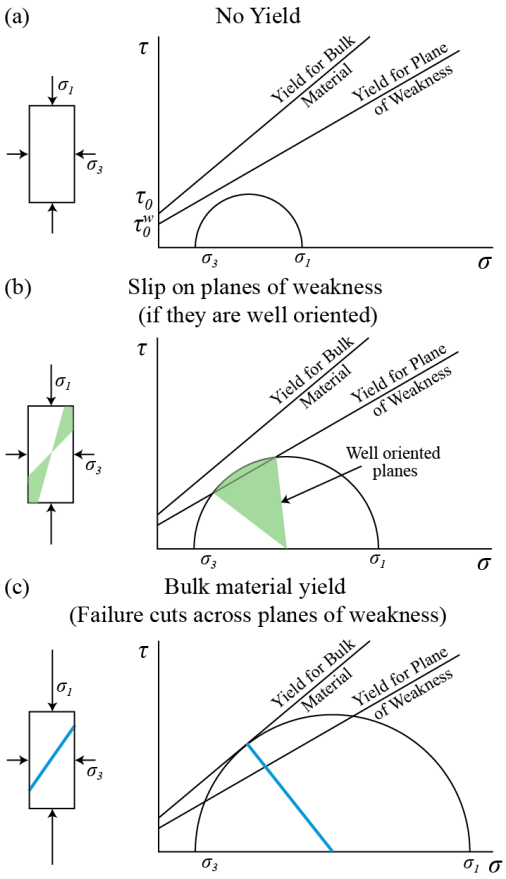

Fig. 5. Plane of weakness failure modes: (a) when stresses are low no failure occurs on the weak plane or through the bulk material; (b) if the weak plane is well oriented an increase in stress results in sliding on the weak plane; (c) if weak plane is not well oriented a further increase in stress results in bulk material failure.

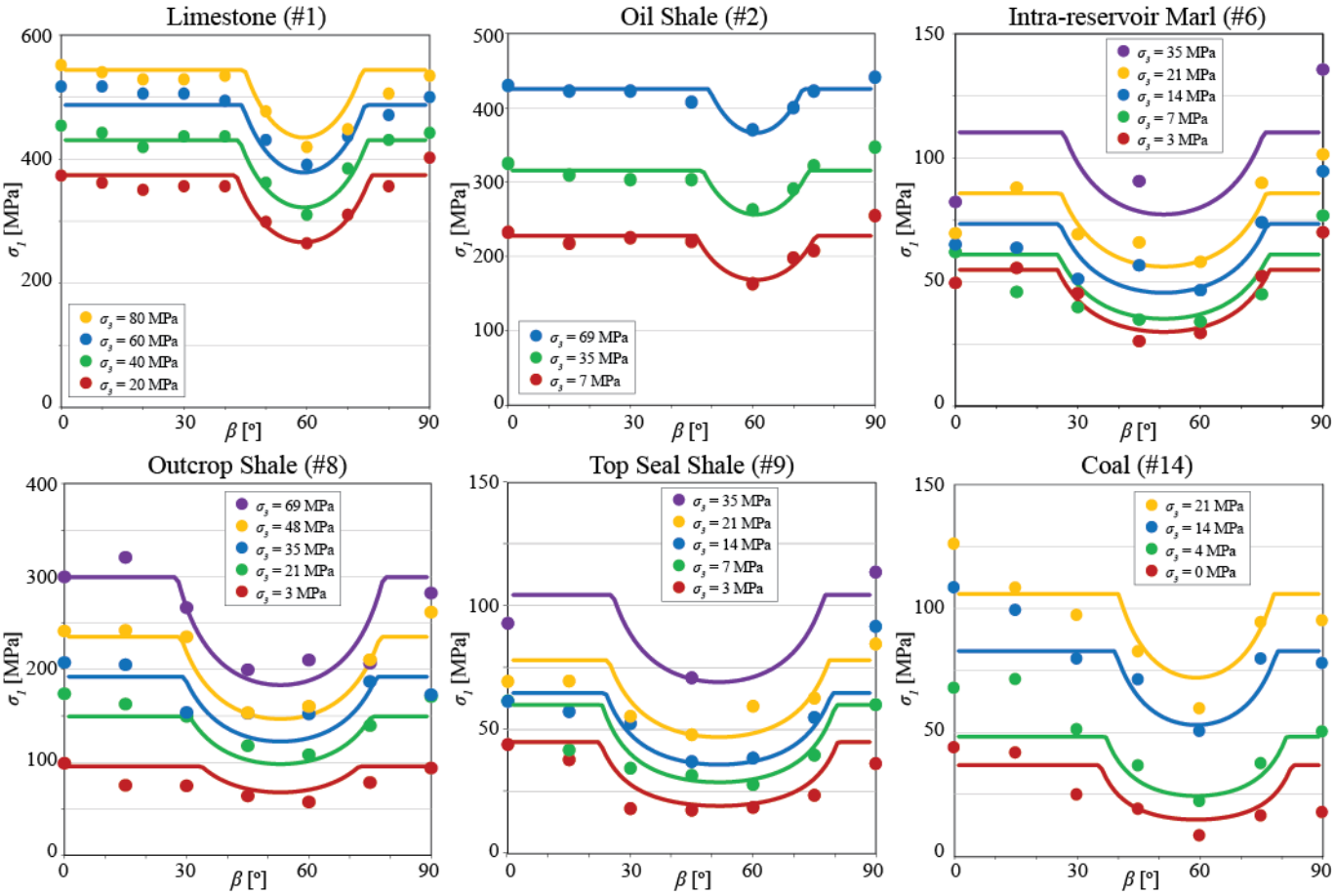

Fig. 6. Single plane of weakness "SPW" model fit (solid lines) to laboratory data (points) for 6 database lithologies.

$$\sigma_1 = \sigma_3 + \frac{2(\tau_0 + \sigma_3 \tan\varphi^w)}{(1 - \tan\varphi^w \cot\beta)\sin 2\beta} \qquad (4)$$

Failure will occur in the bulk material based on the same failure criterion as the weak plane (Eq. 1) such that the maximum principal stress that can be sustained is:

$$\sigma_1 = 2\tau_0^b \frac{\cos\varphi^b}{1 - \sin\varphi^b} + \sigma_3 \frac{1 + \sin\varphi^b}{1 - \sin\varphi^b} \qquad (5)$$

The maximum compressive stress that the rock specimen can undergo for a given orientation angle "β" is the lesser of Eq. 4 and Eq. 5. Therefore "SPW" model fits to experimental data as shown in Fig. 6 exhibit distinct "shoulders" where failure occurs in the bulk material and a "U-shaped" dip where failure occurs on the weak plane with a minimum value at:

$$\beta_{\min}^w = \frac{1}{2}\tan^{-1}(\cot\varphi^w) \qquad (6)$$

To fit this model to experimental strength measurements we first estimate which orientation angles "β" have peak strengths associated with plane of weakness failure and perform a linear regression on strength data for all other orientations to arrive at an average bulk cohesion and friction angle. Plane of weakness cohesion and friction angle values are then determined by minimizing the sum of the squares of all remaining residuals (measured minus modeled strengths) to achieve a best fit with laboratory data. As shown in Fig. 6 we find that the minimum strength value occurs at $\beta_{min}^w > 45°$ for all lithologies and generally occurs at $\beta_{min}^w \approx 60°$. The "SPW" model is a very good representation of the limestone and oil shale data. This is mainly due to the observed uniformity in strength w.r.t. orientation angle for bulk material failure (shearing through planes of weakness). An important general observation derived from all database lithologies is that, because test material is markedly inhomogeneous, between-sample variability for a given lithology is much greater than generally observed in more homogeneous rock types. This effect was quantified by McGill & Raney [25] during anisotropic strength testing of laminated dolomitic limestone (database lithology #1). Using multiple-regression analysis they estimated that about 25% of the variability in compressive strength was directly related to confining pressure, 25% to orientation angle and 10% to strain rate, such that the remainder (nearly 40% of the total) was not related to any of the experimental variables but rather to material inhomogeneity (plus experimental error).

4.2. *Variable Cohesive Strength (periodic)*

In the variable cohesive strength "VCS" [38] formulation there is no distinction between failure of a weak plane and failure through the bulk material. Therefore there is no abrupt change in the model strength w.r.t. orientation angle (as dictated by the "SPW" model, see Fig. 6). The "VCS" model has a continuous variation in cohesive strength "τ_0^c" w.r.t. "β" however the friction angle "φ^c" is assumed to be independent of direction. To achieve periodic variation a cosine function is used such that the material strength criterion is defined by the equations:

$$|\tau| = \tau_0^c + \sigma \tan \varphi^c \tag{7}$$

$$\tau_0^c = A - B \cos\left(2(\beta - \beta_{min}^c)\right) \tag{8}$$

where "A" and "B" are fitting parameters and "β_{min}^c" is the orientation angle at which there is a minimum in the strength data. From the "SPW" fits and an examination of the laboratory data we know that "β_{min}^c" is always greater than 45°. Since a cosine function is used to fit the data and the minimum is at a point ≥45° the strength at β=0° must be larger than that at β=90°. This is a constraint placed by the model that does not represent the observed variation in strength for all database lithologies. In Section 4.3 we discuss a modification to the "VCS" model that allows for the strength at β=90° to be greater than that at β=0°. The "VCS" fit to experimental data is obtained by first setting the constant friction angle "φ^c" equal to the friction angle derived from orientated core measurements at β=0°. The function minimum "β_{min}^c" is then determined using:

$$\beta_{min}^c = 45° + \frac{1}{2}\varphi^c \tag{9}$$

Following quantification of "φ^c" and "β_{min}^c" empirical parameters "A" and "B" are derived using least squares minimization. "VCS" model fits to experimentally-derived Mohr-Coulomb strength parameters for 5 database lithologies are shown in Fig. 7. Experimentally-determined cohesive strength exhibits a fairly systematic continuous variation with orientation angle. The periodic "VCS" model captures this variation to some degree with a function minimum lying between $45^o \leq \beta \leq 60^o$ with the proviso that strength at β=90° is always less than that at β=0°. Compared to the cohesive strength data, friction angle appears to exhibit little or no systematic variation w.r.t. orientation angle "β." This is most likely the result of pronounced between-sample variability for a given lithology due to the markedly inhomogeneous nature of all anisotropic database rocks. This observation tends to support the use of a constant friction angle "φ^c" (as opposed to implementing periodic variation) for such anisotropic rocks.

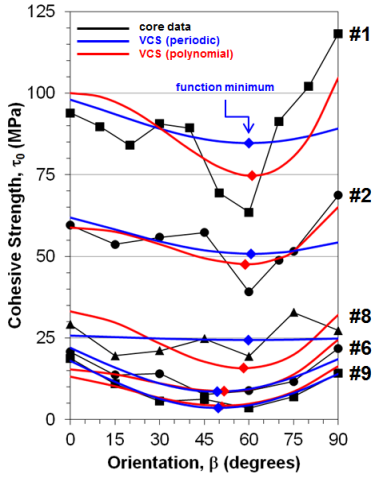

(a)

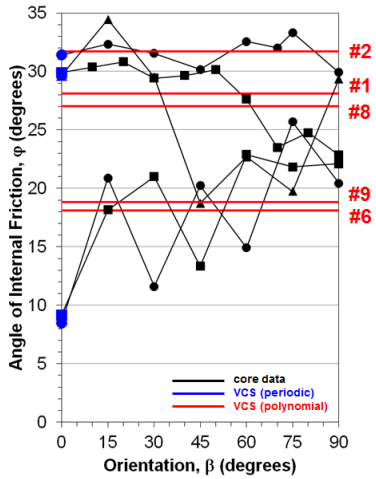

(b)

Fig. 7. Variable cohesive strength model fits ("VCS" periodic in blue, modified "VCS" in red) to core-derived Mohr-Coulomb strength parameters (in black): (a) cohesive strength; (b) internal friction angle.

4.3. *Variable Cohesive Strength (polynomial)*

The third model that we consider is a modified version of the periodic "VCS" formulation that better accounts for material inhomogeneity (between-sample variability) and is not constrained to consistently represent strength at β=90° less than strength at β=0°. Core-derived strength data for a given orientation angle is first fit using the linear Mohr-Coulomb criterion. As shown in Fig. 8 an automated 3D-surface fitting procedure is then implemented to interpolate between these orientation-dependent linear fits with the constraint that all data must have a common slope in the "σ_1" versus "σ_3" plane equal to the arithmetic mean of all core-derived slopes.

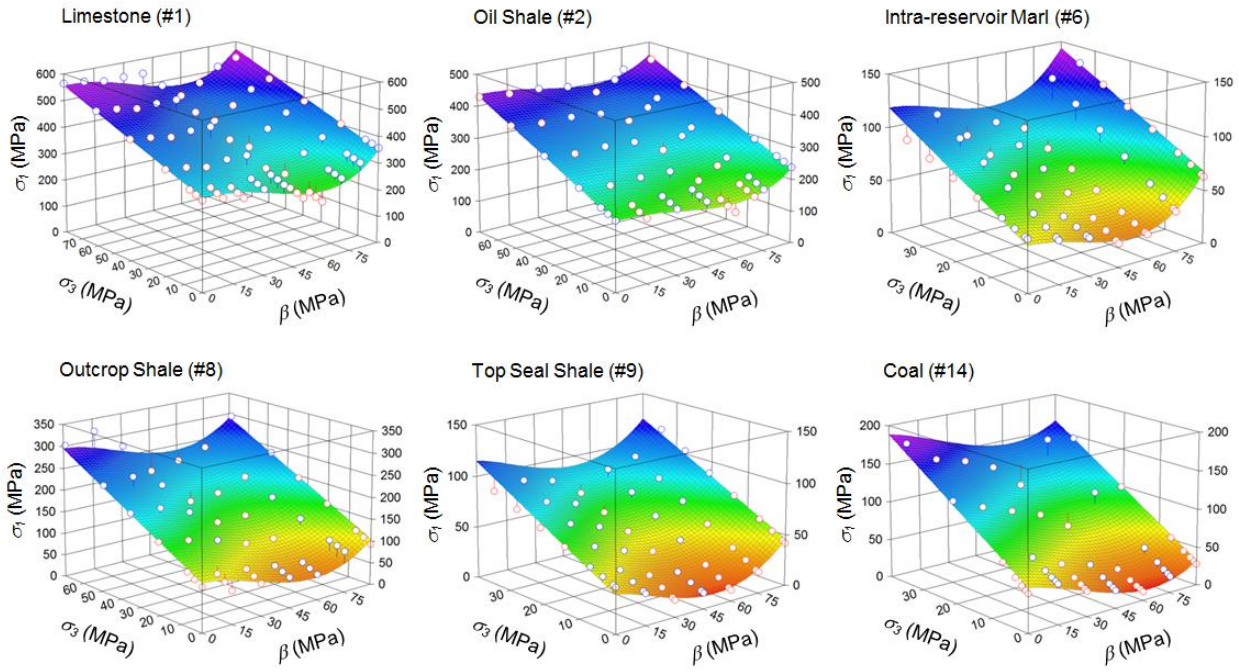

Fig. 8. 3D-surface fits (peak strength σ_1 as a function of confining pressure σ_3 and orientation angle β) to laboratory data for 6 database lithologies.

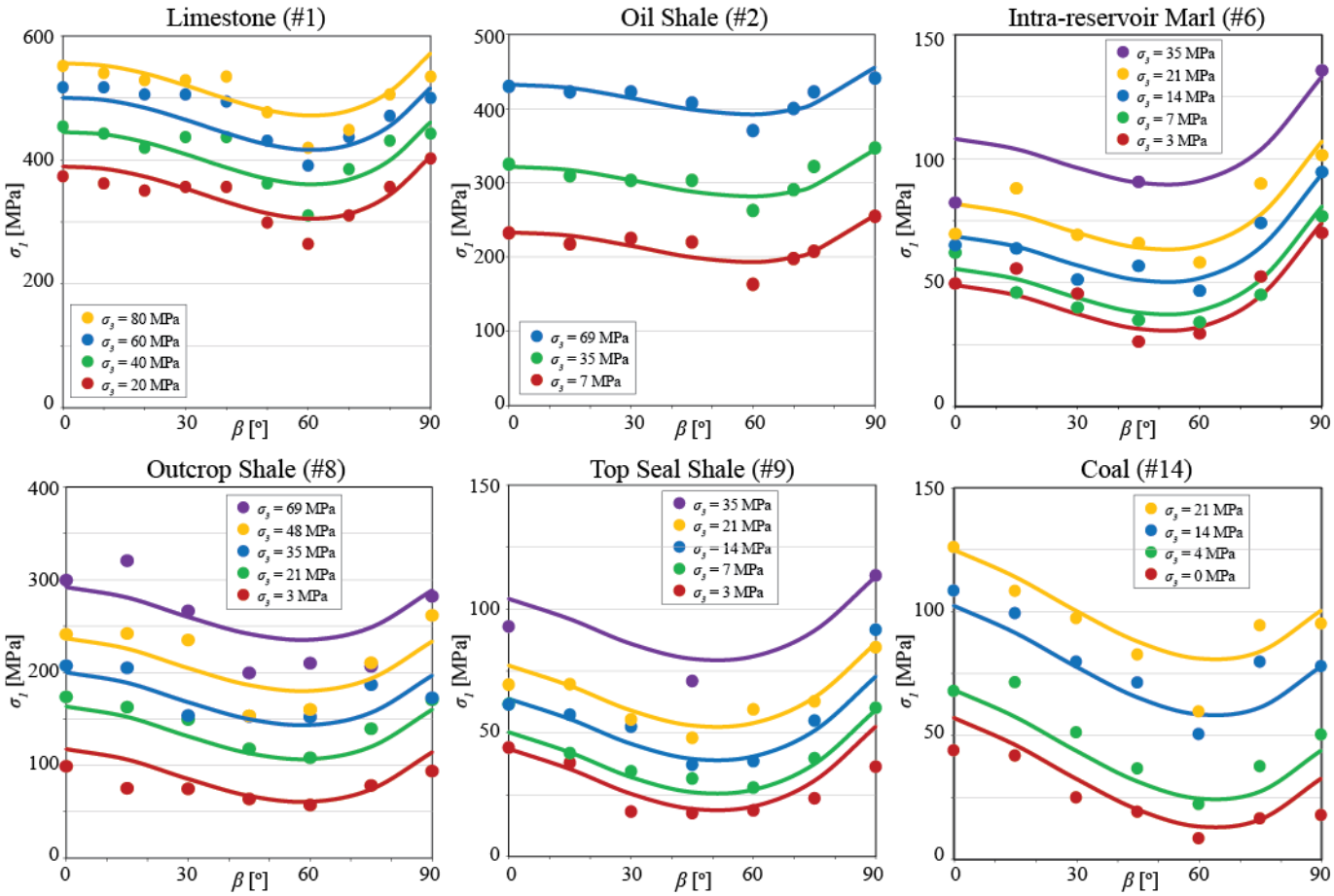

Fig. 9. Modified variable cohesive strength "VCS" model fit (solid lines) to laboratory data (points) for 6 database lithologies.

This tends to smooth out between-sample variability and enables better evaluation of the effect of orientation angle on strength. The modified "VCS" failure criterion is therefore best represented using a friction angle "φ^p" equivalent to the average of all core-derived values as shown in Fig. 7(b). Rather than fitting the cohesive strength data at each orientation angle with a periodic cosine function we observe that a third-order polynomial provides much improved congruency with experimental data. The resulting failure criterion is defined by:

$$|\tau| = \tau_0^p + \sigma \tan \varphi^p \qquad (10)$$

$$\tau_0^p = C\beta^3 + D\beta^2 + E\beta + \tau_0|_{\beta=0^\circ} \qquad (11)$$

$$\bar{\varphi} = \frac{1}{N}\sum_{i=1}^{N} \varphi_i \qquad (12)$$

where "τ_0^p" is the orientation dependent cohesion, "$\tau_0|_{\beta=0^\circ}$" is the cohesive strength at β=0° (conventional compression perpendicular to plane of anisotropy) and the coefficients "C", "D" and "E" are determined by a least squares minimization. The friction angle used in this model "φ^p" is not the core measured friction angle but rather the arithmetic average "$\bar{\varphi}$" of all core-measured friction angles for orientations in the range $0^o \leq \beta \leq 90^o$. Fig. 9 illustrates example fits to experimental data using the modified "VCS" criterion which can be directly compared with the equivalent "SPW" fits as presented in Fig. 6.

5. ANISOTROPIC STRENGTH ESTIMATION

Quantitative assessment of the magnitude of shear strength anisotropy and its potential prediction is hampered by the fact that so few lithologies have been sufficiently characterized experimentally (due to the large number of core tests required) and the inherently inhomogeneous nature of the test materials (between-sample variability) compared with more isotropic rocks. Nevertheless we use our database of experimental measurements and the model fits to evaluate some basic controls related to the development of strength anisotropy in fine-grained rocks. All data tends to support the notion that strength anisotropy is primarily the result of a systematic continuous variation in cohesive strength with orientation angle. By comparison, variability in internal friction angle is much less systematic and most likely the result of material inhomogeneity thus justifying the use of a constant friction angle (as opposed to implementing continuous variation) in anisotropic failure criteria.

Some useful empirical correlations are also evident such as those illustrated in Fig. 10 derived from modified "VCS" fits to experimental data. To first-order we observe that the arithmetic average friction angle "$\bar{\varphi}$" correlates on a near 1:1 basis with the experimentally-measured friction angle "$\varphi|_{\beta=0^\circ}$" derived from conventional triaxial testing with maximum compression perpendicular to the plane of anisotropy. Similarly, the orientation angle "β_{min}" most favorable for shear failure (determined from 3D-surface fitting peak strength as a function of "β" and "σ_3") can be estimated from "$\varphi|_{\beta=0^\circ}$" using Eq. 9.

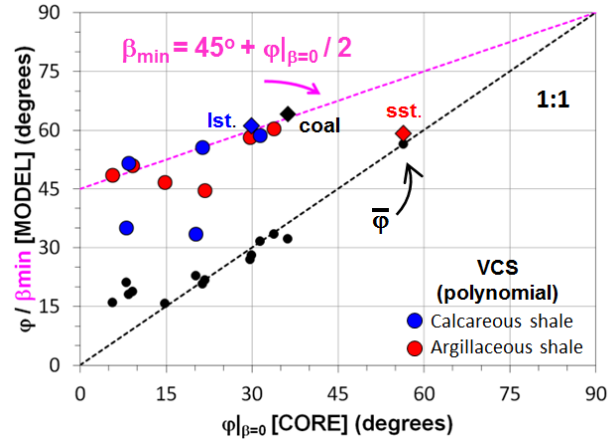

(a)

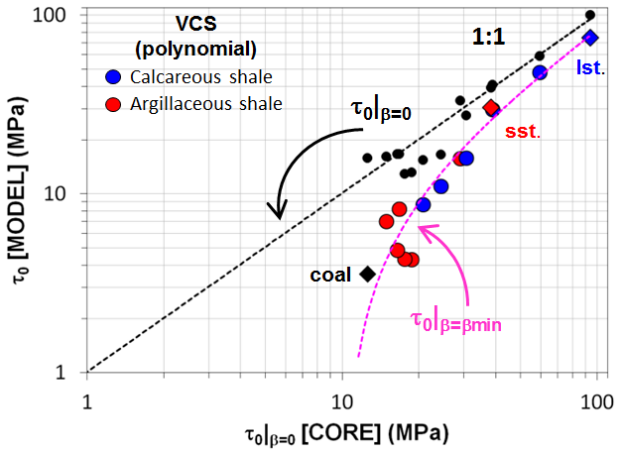

(b)

Fig. 10. Empirical predictive correlations relating "VCS" (polynomial) model parameters to core-derived parameters at β=0°: (a) orientation angle for cohesive strength function minimum; (b) minimum cohesive strength magnitude.

Core-derived and modeled cohesions at the β=0° orientation angle show a strong 1:1 correlation. The functional minimum in cohesive strength "$\tau_0|_{\beta=\beta min}$" also correlates highly with measured "$\tau_0|_{\beta=0^\circ}$" for all lithologies and, interestingly, we note that the difference between the two values increases systematically as cohesive strength measured perpendicular to the plane of anisotropy decreases. Similar results are observed for both the "SPW" and periodic "VCS" formulations but with "τ_0^w" (Eq.1) and "A-B" (Eq.8) replacing "$\tau_0|_{\beta=\beta min}$" respectively.

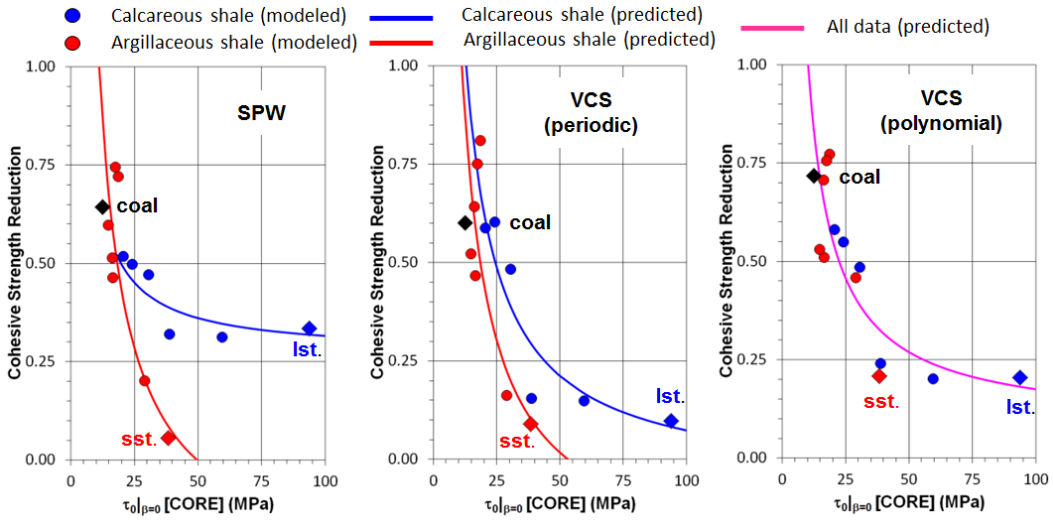

Fig. 11. Cohesive strength reduction (modeled and predicted) for 14 database lithotypes as a function of cohesive strength measured at $\beta = 0^o$.

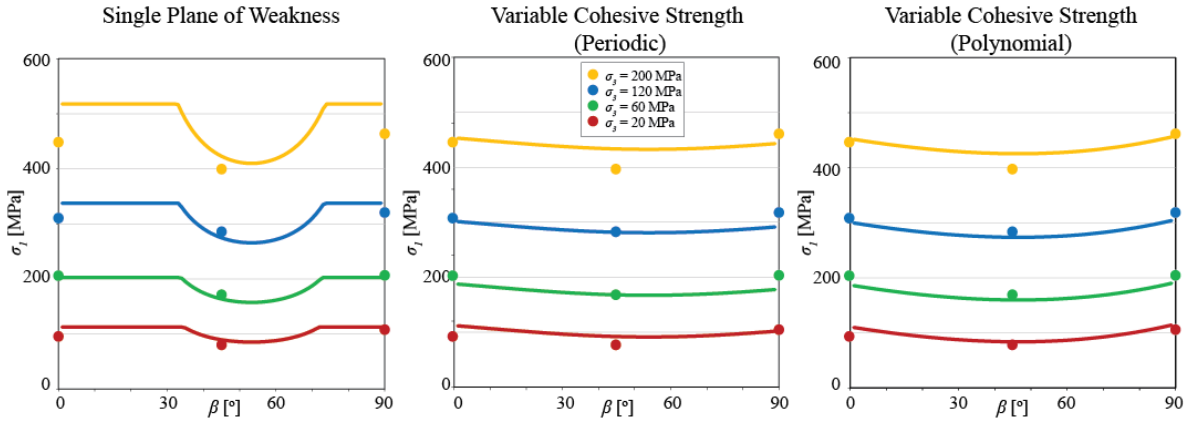

Fig. 12. Predicted model fits (lines) to measured Wilcox shale strength data evaluated at β=0, 45 and 90^o orientations (points).

To quantify the magnitude of strength anisotropy we postulate a "cohesive strength reduction factor" (*CSR*) representing the normalized strength difference associated with shearing across (trans-laminar) versus shear within (intra-laminar) the plane of anisotropy:

$$CSR = \frac{\tau_0|_{\beta=0^\circ}^{core} - \tau_0|_{\beta=\beta_{min}}^{model}}{\tau_0|_{\beta=0^\circ}^{core}} \qquad (13)$$

Cohesive strength reduction as a function of core-derived cohesion measured at β=0^o exhibits significant model dependency as shown in Fig. 11 (points represent model-dependent "*CSR*" values and lines are predictions derived from empirical fits to minimum cohesive strength). However, systematic "*CSR*" decrease associated with increasing "$\tau_0|_{\beta=0}$" magnitude is common to all. Although model predictions are projected upwards to a "*CSR*" magnitude of 1 (implying zero intra-laminar strength) we note that this is an extrapolation and that more low strength measurements at $\tau_0|_{\beta=0}$ ≤10MPa should be performed. Focusing on the modified "VCS" formulation we observe that slip on weak bedding/lamination planes reduces the cohesive strength of sandstone, limestone and oil shale samples by ≈20-25% whereas calcareous and argillaceous shales (plus coal) exhibit ≈45-80% decrease. Thus petrophysical models for predicting rock strength from wireline logs (calibrated from measurements conducted perpendicular to bedding e.g. Crawford *et al* [45]) may offer potential for estimating the magnitude of strength reduction likely to be encountered in anisotropic formations. An example prediction of strength variation with orientation angle is illustrated in Fig. 12 for triaxial compression testing of Wilcox shale as reported by Ibanez & Kronenberg [21]. Core derived cohesion and friction angle at β=0° ($\tau_0|_{\beta=0^\circ}^{core} = 26.3$ MPa; $\varphi|_{\beta=0^\circ}^{core} = 18.1°$) are used to estimate anisotropic strength model coefficients via empirical correlations. This technique could aid in extrapolating strength versus orientation angle data when only a limited number of orientated plugs are available for testing (e.g. Ewy *et al* [46]).

6. CONCLUSIONS

- We have compiled a database of ≈400 orientated triaxially compressive failure tests conducted on 14 strongly anisotropic rocks: 6 argillaceous shales; 3 calcareous marls; 2 oil shales; 1 limestone; 1 sandstone; and 1 coal.
- All anisotropic strength data has been analyzed using both discontinuous single plane of weakness and continuously variable strength models.
- The magnitude of strength anisotropy for a given lithology is shown to depend on the particular model formulation used to analyze experimental data.
- Model fits to experimental data tend to support the notion that strength anisotropy is primarily the result of a systematic continuous variation in cohesive strength with orientation angle.
- Variability in internal friction is much less systematic and most likely the result of material inhomogeneity, thus justifying the use of a constant friction angle in anisotropic failure criteria.
- Slip on weak bedding/lamination planes is observed to reduce the cohesive strength of sandstone, limestone and oil shale samples by ≈20-25% whereas calcareous and argillaceous shales (plus coal) exhibit ≈45-80% decrease, such that higher reduction (greater strength anisotropy) is observed in the weaker fine-grained rocks.

ACKNOWLEDGEMENTS

We thank the management of ExxonMobil (EMURC, EMDC, EMADOPCL) and ZADCO for permission to publish this study. J.D. Rice and D.W. Webb are gratefully acknowledged for conducting all in-house laboratory testing.

REFERENCES

1. Sondergeld, C.H. and C.S. Rai. 2011. Elastic anisotropy of shale. *The Leading Edge* March 2011.
2. Cholach, P.Y. and D.R. Schmitt. 2003. Intrinsic anisotropy of shales. In *Proceedings of the Annual Meeting of the Society of Exploration Geophysicists, Dallas, 26-31 October 2003*.
3. Jones, L.E.A. and H.F. Wang. 1981. Ultrasonic velocities in Cretaceous shales from the Williston basin. *Geophysics* 46(3): 288-297.
4. Hornby, B.E. 1998. Experimental laboratory determination of the dynamic elastic properties of wet, drained shales. *J. Geophys. Res.* 103(B12): 29945-29964.
5. Sayers, C.M. 2005. Seismic anisotropy of shales. *Geophysical Prospecting* 53(5): 667-676.
6. Thomsen, L. 1986. Weak elastic anisotropy. *Geophysics* 51(10): 1954-1966.
7. Lonardelli, I., H.-R. Wenk and Y. Ren. 2007. Preferred orientation and elastic anisotropy in shales. *Geophysics* 72(2): D33-D40.
8. Kaarsberg, E.A. 1959. Introductory studies of natural and artificial argillaceous aggregates by sound-propagation and X-ray diffraction methods. *J. Geol.* 67: 447-472.
9. Vernik, L. 1993. Microcrack-induced versus intrinsic elastic anisotropy in mature HC-source shales. *Geophysics* 58(11): 1703-1706.
10. Sayers, C.M. 1999. Stress-dependent seismic anisotropy of shales. *Geophysics* 64(1): 93-98.
11. Schoenberg, M., F. Muir and C.M. Sayers. 1996. Introducing ANNIE: a simple three-parameter anisotropic velocity model for shales. *J. Seis. Expl*. 5: 35-49.
12. Vernik, L. and A. Nur. 1992. Ultrasonic velocity and anisotropy of hydrocarbon source rocks. *Geophysics* 57(5): 727-735.
13. McLamore, R.T. and K.E. Gray. 1967. A strength criterion for anisotropic rocks based upon experimental observations. In *Proceedings of the Annual Meeting of the American Institute of Mining, Metallurgical and Petroleum Engineers, Los Angeles, 19-23 February 1967.*
14. Donath, F.A. 1964. Strength variations and deformational behavior in anisotropic rock. In *State of Stress in the Earth's Crust*, ed. W.R. Judd, 281-297.
15. Attewell, P.B. and M.R. Sandford. 1974. Intrinsic shear strength of a brittle, anisotropic rock – I, Experimental and mechanical interpretation. *Int. J. Rock Mech. Min. Sci*. 11: 423-430.
16. Cho, J.-W., H. Kim, K.-B. Min and S. Jeon. 2011. An experimental study on deformation and strength anisotropy of transversely isotropic rocks in Korea. In *Proceedings of the 12th International Congress on Rock Mechanics, Beijing, 18-21 October 2011*.
17. Nasseri, M.H.B., K.S. Rao and T. Ramamurthy. 2003. Anisotropic strength and deformational behavior of Himalayan schists. *Int. J. Rock Mech. Min. Sci*. 40(1): 3-23.
18. Shea, W.T. and A.K. Kronenberg. 1993. Strength and anisotropy of foliated rocks with varied mica contents. *J. Struct. Geol.* 15(9): 1097-1121.
19. Niandou, H., J.F. Shao, J.P. Henry and D. Fourmaintraux. 1997. Laboratory investigation of the mechanical behavior of Tournemire shale. *Int. J. Rock Mech. Min. Sci*. 34(1): 3-16.

20. Chenevert, M.E. and C. Gatlin. 1965. Mechanical anisotropies of laminated sedimentary rocks. *Soc. Petrol. Eng. J*. 5: 67-77.

21. Ibanez, W.D. and A.K. Kronenberg. 1993. Experimental deformation of shale: Mechanical properties and microstructural indicators of mechanisms. *Int. J. Rock Mech. Min. Sci. & Geomech. Abstr*. 30(7): 723-734.

22. Ajalloeian, R. and G.R. Lashkaripour. 2000. Strength anisotropies in mudrocks. *Bull. Eng. Geol. Env.* 59: 195-199.

23. Attewell, P.B. and I.W. Farmer. 1976. *Principles of Engineering Geology*. 1st ed. London: Chapman & Hall.

24. Whittles, D.N., E. Yasar, D.J. Reddish and P.W. Lloyd. 2002. Anisotropic strength and stiffness properties of some UK Coal Measure siltstones. *Q. J. Eng. Geol. Hydro*. 35: 155-166.

25. McGill, G.E. and J.A. Raney. 1970. Experimental study of faulting in an anisotropic, inhomogeneous dolomitic limestone. *Geol. Soc. America Bull*. 81: 2949-2958.

26. Pomeroy, C.D., D.W. Hobbs and A. Mahmoud. 1971. The effect of weakness-plane orientation on the fracture of Barnsley Hards by triaxial compression. *Int. J. Rock Mech. Min. Sci*. 8: 227-238.

27. Cooke, M.L. and D.D. Pollard. Bedding-plane slip in initial stages of fault-related folding. 1997. *J. Struct. Geol.* 19(3-4): 567-581.

28. Gazaniol, D., T. Forsans, M.J.F. Boisson and J.-M. Piau. 1995. Wellbore failure mechanisms in shales: Prediction and prevention. *J. Pet. Tech*. July 1995: 589-595.

29. Ottesen, S. 2010. Wellbore stability in fractured rock. In *Proceedings of the IADC/SPE Drilling Conference, New Orleans, 2-4 February 2010*.

30. Willson, S.M., S.T. Edwards, A. Crook, A. Bere, D. Moos, P. Peska and N. Last. 2007. Assuring stability in extended-reach wells – Analyses, practices and mitigations. In *Proceedings of the IADC/SPE Drilling Conference, Amsterdam, 20-22 February 2007*.

31. Brehm, A., C. Ward, D. Bradford and G. Riddle. 2006. Optimizing a deepwater susbsalt drilling program by evaluating anisotropic rock strength effects on wellbore stability and near-wellbore stress effects on the fracture gradient. In *Proceedings of the IADC/SPE Drilling Conference, Miami, 21-23 February 2006*.

32. Lang, J., S. Li and J. Zhang. 2011. Wellbore stability modeling and real-time surveillance for deepwater drilling to weak bedding planes and depleted reservoirs. In *Proceedings of the IADC/SPE Drilling Conference, Amsterdam, 1-3 March 2011*.

33. Gallant, C., J. Zhang, C.A. Wolfe, J. Freeman, T. Al-Bazali and M. Reese. 2007. Wellbore stability considerations for drilling high-angle wells through finely laminated shale: A case study from Terra Nova. In *Proceedings of the SPE Annual Technical Conference, Anaheim, 20-22 November 2007.*

34. Aadnoy, B., G. Hareland, A. Kustamsi, T. de Freitas and J. Hayes. 2009. Borehole failure related to bedding plane. In *Proceedings 43rd US Rock Mechanics Symposium, Asheville, 28 June – 1 July 2009.*

35. Willson, S.M., N.C. Last, M.D. Zoback and D. Moos. 1999. Drilling in South America: A wellbore stability approach for complex geologic conditions. 1999. In *Proceedings of the SPE Latin American and Caribbean Petroleum Engineering Conference, Caracas, 21-23 April 1999.*

36. Narayanasamy, R., D. Barr and A. Milne. 2010. Wellbore-instability predictions within the Cretaceous mudstones, Clair field, west of Shetlands. *SPE Drilling & Completion* December 2010: 518-529.

37. Duveau, G., J.F. Shao and J.P. Henry. 1998. Assessment of some failure criteria for strongly anisotropic rocks. *Mech. Cohes-frict. Mater*. 3: 1-26.

38. Jaeger, J.C. 1960. Shear failure of anisotropic rocks. *Geol. Mag*. 97: 65-72.

39. Walsh, J.B. and W.F. Brace. 1964. A fracture criterion for brittle anisotropic rock. *J. Geophys. Res*. 69(16): 3449-3456.

40. Ramamurthy, T. 1993. Strength and modulus response of anisotropic rocks. In *Comprehensive Rock Engineering Vol. I*, ed. J. Hudson, 313-329.

41. Ramamurthy, T., G.V. Rao and J.A. Singh. 1988. A strength criterion for anisotropic rocks. In *Proceedings of the 5th Australia-New Zealand Conference on Geomechanics, Sydney, 1: 253-257.*

42. Hoek, E. and E.T. Brown. 1980. *Underground Excavations in Rock*. 1st ed. London: The Institution of Mining and Metallurgy.

43. Pariseau, W.G. 1968. Plasticity theory for anisotropic rocks and soil. In *Proceedings 10th US Symposium on Rock Mechanics, Austin, 20-22 May 1968.*

44. Crook, J.L., J.-G. Yu and S.M. Willson. 2002. Development of an orthotropic 3D elastoplastic material model for shale. In *Proceedings of the SPE/ISRM Rock Mechanics Conference, Irving, 20-23 October 2002.*

45. Crawford, B.R., P.J. Gaillot and B. Alramahi. 2010. Petrophysical methodology for predicting compressive strength in siliciclastic "sandstone-to-shale" rocks. In *Proceedings of the 44th US Rock Mechanics Symposium, Salt Lake City, 27-30 June 2010*.

46. Ewy, R.T., C.A. Bovberg and R.J. Stankovic. 2010. Strength anisotropy of mudstones and shales. In *Proceedings of the 44th US Rock Mechanics Symposium, Salt Lake City, 27-30 June 2010*.